Materials Research Proceedings 57 (2025) 208-215 https://doi.org/10.21741/9781644903735-24

# Effect of cyclic loading and thermal stimuli on the shape memory behavior of PLA 3D-printed cellular structures

Desole M.P.[1,a*], Gisario A.[1,b]

[1]Sapienza Università di Roma, Dipartimento di Ingegneria Meccanica e Aerospaziale, Via Eudossiana 18, 001884 Roma, Italy

**Keywords:** Additive Manufacturing, Shape Memory Polymers, Energy Absorption

**Abstract.** This study investigates the shape memory behaviour of PLA 3D printed cellular structures subjected to bending cycles. The focus is on their ability to recover the original shape following the application of a thermal stimulus. Both water and hot air were tested as activation media, with the structures subjected to three alternating cycles of stress and recovery to evaluate their performance. Two structural designs were considered: a topology with negative stiffness, modified to enhance performance and a structure inspired by the spring-loaded crossbow. The latter proved to be more effective, standing out for its mechanical strength and energy absorption capacity. The type of thermal stimulus significantly influences the recovery of the original shape. Specifically, the use of hot air enables localized recovery of the structure, reducing damage to the geometry as a result of cyclic stresses and increasing the energy absorption properties of the structure.

## Introduction

Shape memory polymers (SMPs) are smart materials capable of recovering their original configuration after undergoing permanent deformation, triggered by an external stimulus such as a temperature change. [1,2]. This is known as the shape memory effect (SME) [3]. The integration between SMP and additive manufacturing (AM) also known as 3D printing, has shown significant potential in the realization of complex structures, which would be complicated to achieve through traditional production processes [4]. Traditionally, this technology has been associated with static processes, where the shape and function of objects remain constant over time [5]. The introduction of "4D printing," which incorporates time as a variable in the process [6], marks a significant paradigm shift in the production of complex lattice structures. Polylactic acid (PLA) is a commonly used SMP in 4D printing, enabling the creation of environmentally friendly artifacts [7]. Lattice structures are often studied [8,9] both in mechanical terms [10] and as energy absorbers [11]. Research on these structures frequently focuses on compression [12,13] and impact loads [14,15], whereas studies on bending behavior are more limited. Generally, these structures are analyzed in terms of flexural stiffness [16] and energy absorption capacity [17], but without investigating cyclic loading. The only study that examines three-point cyclic bending stress [18], does not delve into energy absorption capacity. Moreover, no comparisons between thermal stimuli have been conducted, nor has the influence of the type of thermal stimulus on energy absorption and shape recovery been analyzed. The most commonly used thermal stimulus is immersion in hot water [19,20]; however, one of the main issues associated with this method is the hydrostatic force exerted on the geometry during immersion [21]. Additionally, heating is not applied in a localized manner but affects the entire structure instead of focusing solely on the deformed area. To address these challenges, a possible solution is the application of a thermal stimulus using hot air, which allows for more targeted heating control while reducing unwanted effects related to hydrostatic force. The aim of this study is to analyze the behavior of two types of cellular structures made of PLA, fabricated using the Fusion Deposition Modeling technology, subjected to cyclic bending

Content from this work may be used under the terms of the Creative Commons Attribution 3.0 license. Any further distribution of this work must maintain attribution to the author(s) and the title of the work, journal citation and DOI. Published under license by Materials Research Forum LLC.

Materials Research Proceedings 57 (2025) 208-215 https://doi.org/10.21741/9781644903735-24

loads while investigating shape recovery under two different thermal stimuli: water and hot air. The analyzed geometries are classified into two main categories: one characterized by negative stiffness and the other inspired by a leaf spring. The structures undergo three loading cycles, during which elastic recovery and shape restoration are observed. This analysis enables their characterization from both a mechanical standpoint and in terms of energy absorption capacity. The best-performing structure is then tested with a different thermal stimulus, transitioning from water to hot air. Applying hot air to the deformed area allows for localized restoration, reducing geometric damage caused by cyclic loading and improving the structure's energy absorption properties.

## Material and method

*Material and geometry design*

The analyzed structures were fabricated using non-technical PLA filament produced by Ultimaker (Utrecht, Netherlands), with a diameter of 2.85 ± 0.10 mm. This material is frequently used in 4D printing as a shape memory material [22]. The geometries include a negative-stiffness type, inspired by an existing design in the literature [23] and a leaf spring-based design. In the first case, the structure incorporates an ellipsoidal element with its major axis parallel to the specimen length, replacing the traditional vertical rigid element. This modification aims to extend the elastic phase of the structure and reduce force concentration along the cell edges. The second geometry is inspired by the leaf spring, a well-known configuration for its high mechanical resistance and energy absorption capacity [24]. Figure 1 shows the CAD models of the examined structures, designed using Autodesk Inventor 2024. The dimensions were defined following ISO 178:2019 standards. To facilitate the inclusion of hydrophilic support material in Butene Diol Vinyl Alcohol Copolymer (BVOH) and prevent direct contact between the heated bed and the printed pattern, a 1 mm-thick step was added. The densities of the NS_Spring and Leaf_Spring structures are 27% and 30%, respectively.

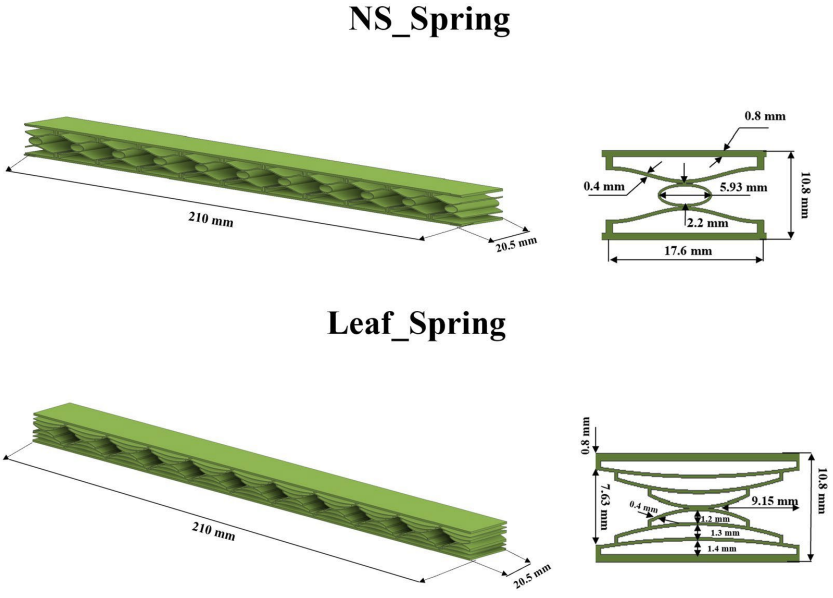



*Figure 1. CAD model of the NS_Spring (a) and Leaf_Spring (b) structures.*

*Manufacturing process*

The samples were produced using FDM technology with an Ultimaker S5 3D printer. The "Ultimaker Care" software was used to set the printing parameters. The printing temperature was set to 200°C for PLA and 210°C for BVOH, in accordance with the materials' technical specifications. To ensure good mechanical strength, the infill density was set to 100%. The printing speed was maintained at 60 mm/s, a value that provides a good balance between part quality and

production time [25]. The layer thickness was set to 0.2 mm, a choice that allows for an optimal balance between detail resolution and printing speed.

*Bending Test*

The machine used for the three-point bending tests is the Shimadzu "Autograph AGS-X series", equipped with a 5 kN load cell and a maximum guaranteed error of 1%. The bending tests were conducted according to the ISO 178:2019 standard, designed to analyze the three-point flexural strength of plastic materials. This standard defines the support span and provides a range of values for the central punch descent speed, which should be selected based on the test conditions. The tests were performed with a speed of 2 mm/min and a displacement of 16 mm, while the support span was set to 60 mm.

*Springback and shape recovery*

The elastic recovery was measured in terms of variation in the structure's rotation angle and reduction in mid-span height compared to the nominal structure height of 10.8 mm. These measurements were taken using a digital protractor and a vernier caliper, respectively, and were recorded over 35 minutes with a 5-minute interval. The recovery process was conducted for comparison purposes using both hot water and hot air. For hot water, the specimens were immersed at 55°C for 90 seconds, a temperature below the material's glass transition temperature (≈58°C [25]). This temperature proved sufficient due to the slenderness of the geometries. Shape recovery using hot air was performed with a STEINEL 2520E hot air gun [26]. The gun was set to 60°C, with an airflow rate of 50%. To ensure uniform heat application, the device was securely mounted on a support, maintaining a constant 60 mm distance between the nozzle and the structure. For recovery monitoring, a tracking software was used, with two markers placed on the beam-like structure: one at the center to track height variations and one at the extremity to measure the rotation angle.

*Cyclical stress and energy absorption*

Three cycles of bending, elastic recovery, and shape recovery were performed for each structure, totaling three cycles per structure. In the case of the NS_Spring, permanent fractures occurred during the fourth cycle, making further testing impossible. Consequently, only the first three cycles were considered for both configurations. For the calculation of the absorption energy, reference was made to the Specific Energy Absorption (SEA), which represents the ratio of absorbed energy, considered as the underlying area of the bending curve and the mass of the structure [27].

## Results and discussion

*Compression test - 3 Cycles*

Figure 2 presents the Force-Displacement curves for three cycles, respectively, for the NS_Spring and Leaf_Spring structures. In the case of NS_Spring, the structure exhibits maximum loads of approximately 50 N in the first cycle, with lower values in the subsequent cycles. Despite the geometrical modifications, which extended the elastic phase and reduced stress concentration compared to the reference structure in the literature [18], its mechanical resistance remains limited. By the third cycle, a decline in resistance is observed due to damage at the layer-to-sinusoid connection, leading to a 35% load drop. Conversely, the Leaf_Spring structure demonstrates a higher maximum load than NS_Spring across all three cycles, consistently exceeding 150 N. Its plastic yielding is more controlled, with limited structural damage, primarily due to its higher density.

Materials Research Proceedings 57 (2025) 208-215 https://doi.org/10.21741/9781644903735-24

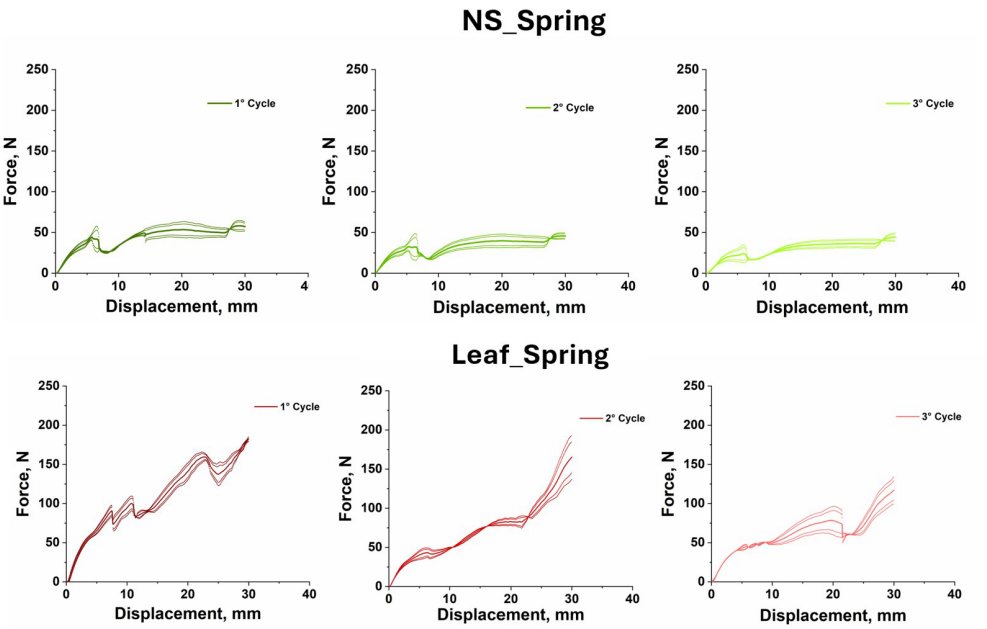



*Figure 2. Curve Force-Displacement 3 Cycles*

*Springback - 3 Cycles*

Figure 3 illustrates the average trend of elastic recovery for the analyzed geometries, expressed in terms of rotation angle and mid-span height. For the NS_Spring, the angle recovery is nearly complete across all three loading cycles, with a final value of approximately 3°. In terms of height, the final value reaches around 8 mm, showing a progressive increase from the first to the third cycle. Conversely, the Leaf Spring structure exhibits less effective elastic recovery. The final angle in the first cycle is 17°, increasing progressively up to 28° in the third cycle. A similar trend is observed for height, with final values ranging between 6 and 7 mm from the first to the third cycle.

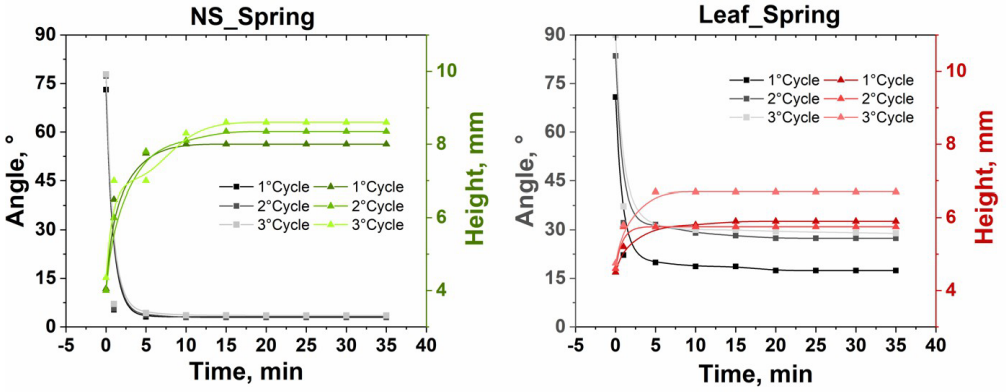



*Figure 3. Springback 3 Cycles*

*Shape recovery - 3 Cycles*

Figure 4 illustrates the average shape recovery of the analyzed geometries, expressed in terms of rotation angle and mid-span height. The results confirm the observations from the elastic recovery analysis, highlighting consistency in the deformation recovery data. The NS_Spring exhibits complete angle recovery, demonstrating excellent repeatability of the phenomenon. In terms of height, the recovery is nearly total, reaching values of approximately 10 mm. Contrary to [23], this study shows that targeted geometric changes improve angular recovery even in the presence of repeated cycles. Conversely, the Leaf Spring structure shows greater difficulty in angle recovery, achieving only 2.5° in the third cycle, likely due to the effect of hydrostatic force and the density

Materials Research Proceedings 57 (2025) 208-215 https://doi.org/10.21741/9781644903735-24

of the structure. However, height recovery proves to be more effective, with final values exceeding 8 mm across all three cycles.

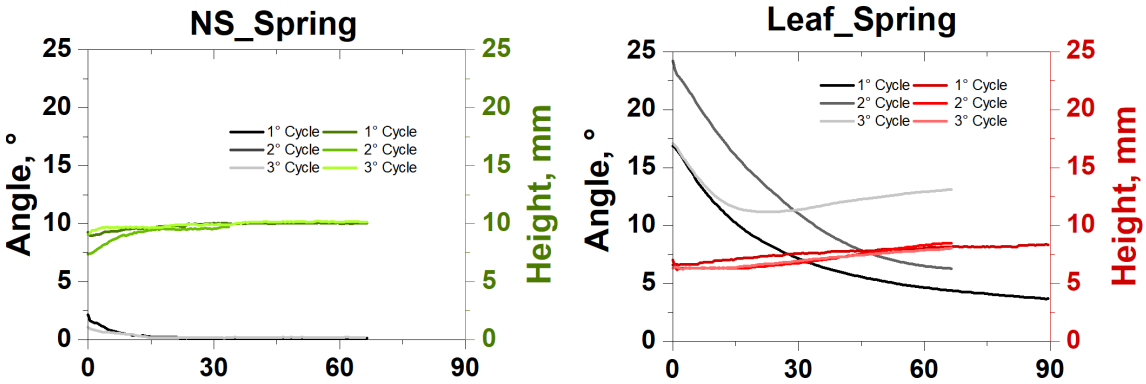



*Figure 4. Angle and height recovery 3 Cicli*

Specifically, the NS_Spring demonstrates a highly effective angle recovery, although the height restoration in the third cycle appears to be limited.

Conversely, the Leaf Spring exhibits an almost constant height recovery across all cycles but struggles more with angle recovery.

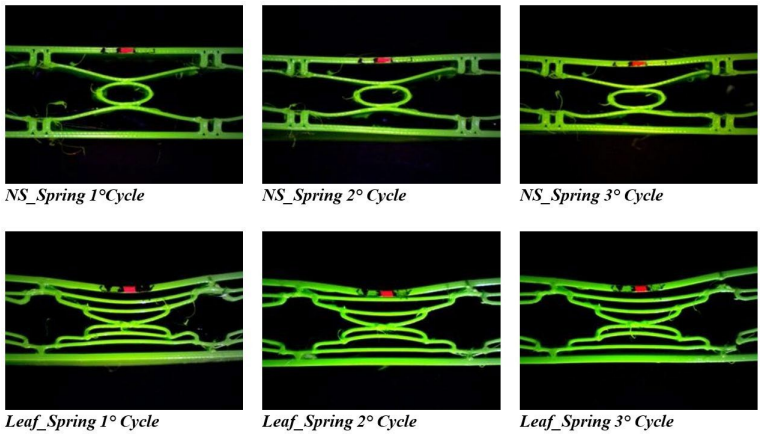



*Figure 5. Visual analysis of the structures after three cycles*

*Energy Absorption – shape recovery hot air*

The energy absorption was measured using the specific energy absorption (SEA) parameter [28], which represents the ratio between the energy absorbed during the bending test and the mass of the structure. Figure 6 presents the average energy absorption values, showing that the Leaf_Spring structure exhibits a higher energy absorption capacity, with values ranging from 194 mJ/g in the first cycle to 112.3 mJ/g in the third cycle. In contrast, the NS_Spring structure demonstrates lower energy absorption compared to the Leaf_Spring. However, it shows a moderate energy reduction of approximately 32%, due to its more limited plastic deformation. In contrast to previous studies focusing on compression tests [10,12,16], the results show that the Leaf_Spring structure, thanks to its symmetrical and flexible geometry, is suitable for repeated cycles without obvious damage up to the third cycle. The energy absorbed remains above 100 mJ/g, making it suitable for cyclic applications such as reusable packaging or active devices.

Materials Research Proceedings 57 (2025) 208-215 https://doi.org/10.21741/9781644903735-24

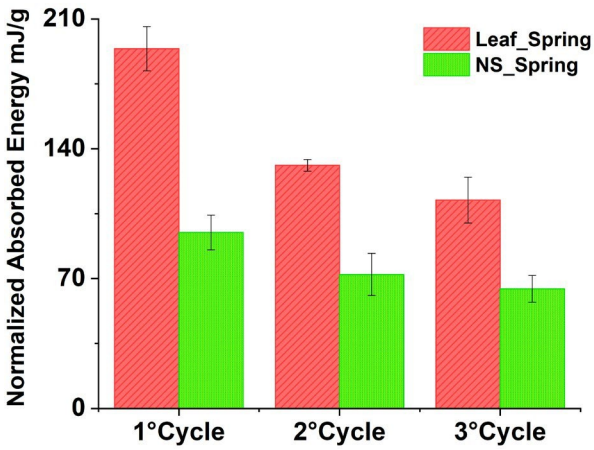



*Figure 6. Energy Absorption with Recovery Using Hot Water*

*Leaf_Spring Energy Absorption – Comparison in shape recovery water/hot air*

Figure 7 shows the methodology used for stress cycles (a), the comparison of absorption energy between water and hot air (b) and a visual analysis of the structure at the end of the third cycle, with recovery by water and hot air. Three stress cycles were usually performed, followed by elastic return and shape recovery, with a warm air recovery following the same principle as hot water. For all three cycles of stress, elastic return and shape recovery, an increase in the absorption energy is observed if the recovery is performed with hot air, with variations of 11% in the first and second cycle and 9% in the third cycle. This behaviour can be explained by the increased mechanical strength of the structure, resulting from a localized rather than global shape recovery.

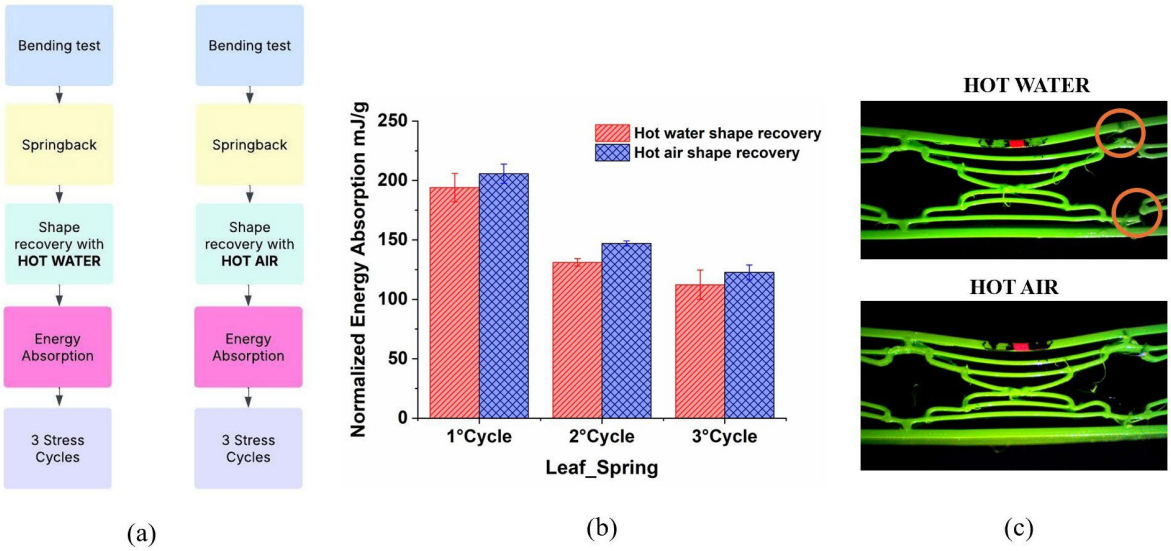



*Figure 7. Energy Absorption with Recovery Using Hot Air*

## Conclusions

The present study analyzed the bending behavior of two cellular structures made of PLA, with different densities, optimized through targeted modifications to improve mechanical resistance and energy absorption capacity. The structures underwent three loading cycles, including bending, elastic recovery, and shape recovery using hot water, to evaluate their mechanical resistance and energy absorption. From the analysis, the NS_Spring, characterized by lower density, exhibited lower mechanical resistance but demonstrated more effective elastic recovery and better shape recovery. In contrast, the Leaf_Spring, inspired by the leaf spring, showed higher mechanical

resistance and better energy absorption. As a result, the Leaf_Spring structure was subjected to three additional loading cycles with shape recovery using hot air, to assess the effect of different thermal stimuli. The hot air stimulus induced localized recovery, unlike hot water, which acts more uniformly. This approach enhanced the structure's performance, increasing energy absorption by approximately 10% on average, while also eliminating the hydrostatic force issue typically associated with hot water recovery.

**References**

[1] B. Ch. Kholkhoev *et al.*, «4D-printing of mechanically durable high-temperature shape memory polymer with good irradiation resistance», *Applied Materials Today*, vol. 36, p. 102022, feb. 2024. https://doi.org/10.1016/j.apmt.2023.102022
[2] G. Dixit e P. M. Pandey, «Experimental investigations of temperature-sensitive shape memory polymer composites for 4D printing», *Journal of Thermoplastic Composite Materials*, vol. 38, fasc. 2, pp. 537–563, feb. 2025. https://doi.org/10.1177/08927057241254322
[3] W. Xu, Z. Ping, X. Gong, F. Xie, Y. Liu, e J. Leng, «Self-Healing Polymers Coupling Shape Memory Effect», *Langmuir*, vol. 40, fasc. 31, pp. 15957–15968, ago. 2024. https://doi.org/10.1021/acs.langmuir.4c01369
[4] J. Ukwaththa, S. Herath, e D. P. P. Meddage, «A review of machine learning (ML) and explainable artificial intelligence (XAI) methods in additive manufacturing (3D Printing)», *Materials Today Communications*, vol. 41, p. 110294, dic. 2024. https://doi.org/10.1016/j.mtcomm.2024.110294
[5] G. Ehrmann e A. Ehrmann, «3D printing of shape memory polymers», *Journal of Applied Polymer Science*, vol. 138, fasc. 34, p. 50847, 2021
[6] A. Sadraei e S. M. Naghib, «4D printing of physical stimuli-responsive hydrogels for localized drug delivery and tissue engineering», *Polymer Reviews*, vol. 65, fasc. 1, pp. 104–168, 2025.
[7] E. Rezvani Ghomi *et al.*, «The life cycle assessment for polylactic acid (PLA) to make it a low- carbon material», *Polymers*, vol. 13, fasc. 11, p. 1854, 2021.
[8] J. Wu, W. Wang, e X. Gao, «Design and optimization of conforming lattice structures», *IEEE transactions on visualization and computer graphics*, vol. 27, fasc. 1, pp. 43–56, 2019.
[9] W. Tao e M. C. Leu, «Design of lattice structure for additive manufacturing», presentato al 2016 International Symposium on Flexible Automation (ISFA), IEEE, 2016, pp. 325–332.
[10]M. Munford, U. Hossain, S. Ghouse, e J. R. T. Jeffers, «Prediction of anisotropic mechanical properties for lattice structures», *Additive Manufacturing*, vol. 32, p. 101041, mar. 2020. https://doi.org/10.1016/j.addma.2020.101041
[11]H. Yin, W. Zhang, L. Zhu, F. Meng, J. Liu, e G. Wen, «Review on lattice structures for energy absorption properties», *Composite Structures*, vol. 304, p. 116397, gen. 2023. https://doi.org/10.1016/j.compstruct.2022.116397
[12]P. Xu *et al.*, «Compression behavior of 4D printed metamaterials with various Poisson's ratios», *International Journal of Mechanical Sciences*, vol. 264, p. 108819, feb. 2024. https://doi.org/10.1016/j.ijmecsci.2023.108819
[13]Y. Chen, L. Ye, Y. X. Zhang, e K. Fu, «Compression behaviours of 3D-printed CF/PA metamaterials: Experiment and modelling», *International Journal of Mechanical Sciences*, vol. 206, p. 106634, set. 2021. https://doi.org/10.1016/j.ijmecsci.2021.106634
[14]K. K. Dudek, W. Wolak, R. Gatt, e J. N. Grima, «Impact resistance of composite magnetic metamaterials», *Scientific Reports*, vol. 9, fasc. 1, p. 3963, mar. 2019. https://doi.org/10.1038/s41598-019- 40610-w

[15]L. Meng *et al.*, «Impact resisting mechanism of tension–torsion coupling metamaterials», *International Journal of Mechanical Sciences*, vol. 272, p. 109100, giu. 2024. https://doi.org/10.1016/j.ijmecsci.2024.109100
[16]N. Korshunova *et al.*, «Bending behavior of octet-truss lattice structures: Modelling options, numerical characterization and experimental validation», *Materials & Design*, vol. 205, p. 109693, lug. 2021. https://doi.org/10.1016/j.matdes.2021.109693
[17]H. Jiang, H. Ziegler, Z. Zhang, S. Atre, e Y. Chen, «Bending behavior of 3D printed mechanically robust tubular lattice metamaterials», *Additive Manufacturing*, vol. 50, p. 102565, feb. 2022. https://doi.org/10.1016/j.addma.2021.102565
[18]D. Koske e A. Ehrmann, «Infill designs for 3D-printed shape-memory objects», *Technologies*, vol. 9, fasc. 2, p. 29, 2021.
[19]B. B. Samal, A. Jena, S. K. Varshney, e C. S. Kumar, «FDM 4D printing: A low-cost approach of shape programming and assessing the shape memory properties using angle measurement methods in hot water actuation testing apparatus», *Materials Today: Proceedings*, vol. 101, pp. 7–14, gen. 2024. https://doi.org/10.1016/j.matpr.2023.02.038
[20]J. Wu *et al.*, «Multi-shape active composites by 3D printing of digital shape memory polymers», *Scientific Reports*, vol. 6, fasc. 1, p. 24224, apr. 2016. https://doi.org/10.1038/srep24224.
[21]A. Gisario, M. P. Desole, M. Mehrpouya, e M. Barletta, «Energy absorbing 4D printed meta-sandwich structures: load cycles and shape recovery», *The International Journal of Advanced Manufacturing Technology*, vol. 127, fasc. 3, pp. 1779–1795, 2023.
[22]Y. Wang *et al.*, «Photoresponsive triple shape memory polymers with a self-healing function based on poly (lactic acid)/polycaprolactone blends», *Polymer Testing*, vol. 120, p. 107966, mar. 2023. https://doi.org/10.1016/j.polymertesting.2023.107966
[23]D. Koske e A. Ehrmann, «Advanced infill designs for 3d printed shape-memory components», *Micromachines*, vol. 12, fasc. 10, p. 1225, 2021.
[24]J. Jancirani e H. Assarudeen, «A review on structural analysis and experimental investigation of fiber reinforced composite leaf spring», *Journal of Reinforced Plastics and Composites*, vol. 34, fasc. 2, pp. 95–100, gen. 2015. https://doi.org/10.1177/0731684414564477
[25]Q. Zhao, H. J. Qi, e T. Xie, «Recent progress in shape memory polymer: New behavior, enabling materials, and mechanistic understanding», *Progress in Polymer Science*, vol. 49–50, pp. 79–120, ott. 2015. https://doi.org/10.1016/j.progpolymsci.2015.04.001
[26]Y. Wu, Y. Han, Z. Wei, Y. Xie, J. Yin, e J. Qian, «4D Printing of Chiral Mechanical Metamaterials with Modular Programmability using Shape Memory Polymer», *Advanced Functional Materials*, vol. 33, fasc. 52, p. 2306442, 2023. https://doi.org/10.1002/adfm.202306442
[27]A. Rajput, M. R. Sunny, e A. Sarkar, «Optimization of honeycomb parameters of sandwich composites for energy and specific energy absorption using particle swarm optimization», *Marine Structures*, vol. 92, p. 103498, nov. 2023. https://doi.org/10.1016/j.marstruc.2023.103498
[28]Y. Ji, Z. Gao, W. Chen, H. Huang, M. Li, e X. Li, «Study on the deformation mode and energy absorption characteristics of a corner-enhanced biomimetic spider web hierarchical structure», *Thin- Walled Structures*, vol. 199, p. 111810, giu. 2024. https://doi.org/10.1016/j.tws.2024.111810